Applied Catalysis B: Environmental 200 (2017) 237–245

Contents lists available at ScienceDirect

Applied Catalysis B: Environmental

journal homepage: www.elsevier.com/locate/apcatb

On the performance of a hybrid process to mineralize the herbicide tebuthiuron using a DSA® anode and UVC light: A mechanistic study

Isaac J.S. Montes[a], Bianca F. Silva[b], José M. Aquino[a,*]

[a] Departamento de Química, Universidade Federal de São Carlos, C.P. 676, 13560-970 São Carlos, SP, Brazil
[b] Instituto de Química de Araraquara, Departamento de Química Analítica, Universidade Estadual Paulista, 14800-900 Araraquara, SP, Brazil

ARTICLE INFO

Article history:
Received 29 March 2016
Received in revised form 10 June 2016
Accepted 4 July 2016
Available online 5 July 2016

Keywords:
Mediated oxidation
Synergistic effect
Synthetic organic pollutants
Organochlorine compounds
Mixed oxide anode

ABSTRACT

A hybrid electrochemical and photochemical (HEP) process was used to oxidize and mineralize the herbicide tebuthiuron (TBT), which is a potential contaminant of ground water, using a DSA® anode and UVC light. The electrochemical and photochemical experiments were carried out in flow reactors and the investigated variables were: *i*) power of the Hg lamp (5, 9, 80, and 125 W), *ii*) solution pH (3, 7, 11, and no control), *iii*) NaCl concentration (0, 1, 2, and 4 g L^{-1}), and *iv*) electric current density (10, 20, and 30 mA cm^{-2}). The performance of the oxidation and mineralization process of TBT and its intermediates was assessed by high performance liquid chromatography coupled to mass spectrometry and total organic carbon analyses. The use of a 9 W Hg lamp led to complete oxidation and mineralization of TBT, and its intermediate compounds, from acidic to neutral solutions, independently of the applied electric current density, and with increasing NaCl concentration. High CO_2 conversions were obtained using the HEP process, as the generated intermediates (including an organochlorine) were completely eliminated. TBT removal rates similar to those of an electrochemical experiment using a boron-doped diamond anode were attained using the HEP process, but with higher energy consumption; however, chlorinated carboxylic acids were no longer present in the final treatment stages. The HEP process could be regarded as an advanced oxidation process, being an interesting option to treat effluents contaminated with organics if a proper optimization of the UVC lamp is done.

© 2016 Elsevier B.V. All rights reserved.

1. Introduction

Surface water contamination by distinct synthetic organic compounds (SOC) has become one of the most important problems in this century, because of the SOC recalcitrance towards removal by microorganisms and the increasing scarcity of easily available surface water [1]. A large number of papers have reported on the detection, through liquid chromatography coupled to mass spectrometry [2], of many different classes of SOC in surface water [3], even after treatment at municipal wastewater treatment plants, such as: herbicides, antibiotics, personal care products, and so on [4,5]. In the environment, such compounds can cause severe damage to aquatic and human lives [6], and thus their effects need further investigation. Consequently, there is the necessity to adequately treat effluents, using distinct methods or their combination [7], before disposal in the environment.

A large number of methods to treat effluents containing organic compounds have been described in the literature [8]. The choice of a certain treatment method usually depends on the physical chemical characteristics of the effluent that will be treated [7]. Among those methods, the electrochemical one is the choice when adequate levels of dissolved organic load [9] and conductivity are present in the effluent. The main drawback of electrochemical technology is the use of electrical energy; however, the efficiency of organic compound removal to the electrical energy consumed can be optimized by the choice of adequate electrode materials [10], as well as the combination with another treatment method [11]. Among the available electrode materials, boron-doped diamond has been extensively used to detect many different kinds of organic compounds [12] and treat effluents contaminated with SOC [13], due to the quasi free hydroxyl radicals (HO•) produced from water discharge [14]; however, there are some operational problems associated with this anode, such as the BDD film stability during electrooxidation in the presence of chloride ions (Cl^-) [15,16]. On the other hand, dimensionally stable anodes (DSA®) are electrochemically stable and commercially available [17]. These anodes are mainly used in the presence of Cl^- (with an interest-

* Corresponding author.
E-mail address: jmaquino@ufscar.br (J.M. Aquino).

http://dx.doi.org/10.1016/j.apcatb.2016.07.003
0926-3373/© 2016 Elsevier B.V. All rights reserved.

ing exception [18]) to produce active chlorine oxidants (Cl_2, HOCl, and OCl^-), as the overpotential value for this reaction is low, to oxidize and partially mineralize SOC [19]. Moreover, as the oxidation power of these oxidants is weak in comparison to that of $HO^•$, it is common to irradiate the DSA® surface with ultraviolet (UV) light (generally using high pressure mercury lamps with the most intense line at 254 nm – UVC) to generate electron/hole pairs, with subsequent $HO^•$ generation through the oxidation of water by the hole [20,21]. In parallel, UVC radiation can also promote the homolysis of active chlorine species to generate $HO^•$ and $Cl^•$ [22], leading to significant removal of organic compounds [23,24]. The photolysis of these compounds by UVC radiation is also possible [25] through the decomposition of previously excited organic molecules, or reaction with reactive oxygen species [26,27], to its intermediates or to CO_2. The main negative points of this combined process, which is commonly denominated as "photo-assisted electrochemical process", are the high electrical energy consumption caused by the use of high pressure UV lamps [28], low fluency rate, low ratio of anatase to rutile crystalline phases in the DSA® anode (leading to poor efficiency in the electron/hole pair formation), and possible formation of organochlorine compounds (aromatic or short chain carboxylic acids) [29,30]. All these features have led to uncertainties regarding the electrical energy efficiency of the process and its environmental safety.

Thus, the aim of the present work is to use a combined electrochemical and photochemical process (also called a hybrid electrochemical and photochemical process), without direct UV irradiation of the DSA® surface, to mineralize a synthetic solution containing the herbicide tebuthiuron (TBT), with concomitant identification of the main organic intermediate compounds formed in the process. TBT is largely used in the cultivation of sugar cane, thus being a potential contaminant of soil [31] and surface [32] water. As far as we know, no work in the literature describes the degradation of TBT and the detection of its degradation byproducts using the hybrid system proposed in this work; only electrochemical [33,34] and photo-Fenton [35–38] technologies have been used. The main idea is to use a commercial DSA® anode to electrogenerate active chlorine species (as the Cl^- ion has a higher diffusion coefficient than SOC), which subsequently will undergo homolytic cleavage in the bulk of the solution mediated by UVC radiation emitted by a low power Hg lamp; we intend to prove that this hybrid electrochemical and photochemical process (using a DSA®) is economically feasible and could be described as a hybrid advanced oxidation process. Accordingly, a simple electrochemical flow reactor (without quartz windows) coupled to a photochemical flow reactor will be used and the effect of the following process parameters will be assessed: power of the UV lamp used, current density, solution pH and NaCl concentration. The optimized results in terms of these parameters, as well as the mineralization current efficiency, electrical energy consumption, and extent of total electrochemical combustion (conversion to CO_2) will be compared to those attained using solely the electrochemical method with a BDD anode. In addition, the kinetic parameters of both processes will be compared with those of a theoretical model purely based on a mass transport controlled process.

2. Experimental

2.1. Chemicals

All chemicals, including tebuthiuron (500 g L^{-1} commercial solution, Adama Brasil), Na_2SO_4 (a.r., Qhemis), NaCl (a.r., Qhemis), $Na_2S_2O_3$ (a.r., Qhemis), KI (a.r., Synth), H_3PO_4 (85%, Mallinckrodt), $Na_2S_2O_8$ (a.r., Sigma Aldrich), formic acid (a.r., JT Baker) and acetonitrile (HPLC grade, JT Baker), were used as received. All carboxylic acids were purchased from Sigma Aldrich. Deionized water (Millipore Milli-Q system, resistivity ≥18.2 MΩ cm) was used for the preparation of all solutions.

2.2. Electrochemical and photochemical degradation experiments

A schematic representation of the hybrid electrochemical and photochemical flow system can be seen in Fig. SM 1a, in the Supplementary material file. The electrochemical experiments were carried out in a one-compartment filter-press flow reactor containing a DSA® ($Ti/Ru_{0.3}Ti_{0.7}O_2$ - nominal composition) and two AISI 304 stainless steel plates as anode and cathodes, respectively (see details in Fig. SM 1b in the Supplementary material file). The exposed area of the DSA® anode was 4.16 cm × 2.75 cm (each face), respectively, and the distance between electrodes was around 5 mm. The photochemical process was carried out by irradiation of the electrolyzed solution in the system's reservoir using low and high pressure Hg lamps. The investigated variables and their ranges in the degradation of 100 mg L^{-1} of tebuthiuron (TBT) solutions in aqueous 0.1 M Na_2SO_4 were: *i*) power of commercial Hg lamps (5, 9, 80, and 125 W), *ii*) solution pH (3, 7, 10, and with no control), *iii*) added NaCl concentration (0, 1, 2, and 4 g L^{-1}), and *iv*) current density (10, 20, and 30 mA cm^{-2}). The fluency rate of the Hg lamps was measured with a FieldMaxII radiometer and the obtained values can be seen in Table SM 1, in the Supplementary material file. The solution pH was continuously monitored and kept constant at the desired values by addition of concentrated solutions of H_2SO_4 or NaOH. The flow rate, flow velocity, electrolysis time, and treated solution volume were fixed: 420 L h^{-1}, 0.29 m s^{-1}, 360 min, and 1.0 L, respectively. Before any electrochemical and photochemical experiment and in order to eliminate any adsorbed organic compound on the DSA® surface, this electrode was electrochemically pretreated in 0.1 mol L^{-1} Na_2SO_4 by applying 20 mA cm^{-2} for 15 min. After the optimization of the hybrid electrochemical and photochemical process, its attained dissolved organic matter removal efficiency and electrical energy efficiency were compared to those of an additional solely electrochemical experiment carried out using a boron-doped diamond (BDD) anode. This electrode (boron content of 500 ppm in the BDD film, deposited on a Si substrate) was purchased from NeoCoat SA (Switzerland).

2.3. Analyses

The evolution of the concentration of TBT was monitored by high performance liquid chromatography (HPLC) using a core shell C-18 reversed phase as the stationary phase (150 mm × 4.6 mm, 5 μm particle size, from Phenomenex®) and a mixture of H_2O and acetonitrile (75:25 *V*/*V*) in an isocratic elution mode as the mobile phase, at 1 mL min^{-1}. TBT was detected at 254 nm. The injection volume and temperature of the column were 25 μL and 23 °C, respectively.

Analyses of the intermediate compounds were made every 1 h until 8 h of electrolysis. The 2 mL extracted samples were first frozen and then dried in a lyophilization system (CHRIST alpha 2-4 LD Plus) for 24 h. After this period, the samples were resuspended in 1 mL of acetonitrile and filtered using a 0.22 μm cartridge coupled to a glass syringe. The intermediates formed during the TBT degradation process were determined by liquid chromatography coupled to a mass spectrometer (LC–MS/MS) analyses in a 1200 Agilent Technologies HPLC coupled to a 3200 QTRAP mass spectrometer (QqLIT - Linear Ion Trap Quadrupole LC–MS/MS Mass Spectrometer), AB SCIEX Instruments, operating in a positive mode, and TurboIonSpray ionization. A special software *Lightsight*® 2.3 (Nominal Mass Metabolite ID Software, AB SCIEX) was used to investigate all byproduct possibilities. The application of the software was performed after optimization of the ionization and fragmenta-

tion parameters for the initial compound. The parameters were obtained using a direct infusion of 10 μL min^{-1} of a solution containing TBT (t = 0 h) in acetonitrile. The MS/MS conditions were: curtain gas at 20 psi, ion spray at 5200 V, gas 1 and gas 2 at 50 psi, temperature of 600 °C, declustering potential of 41 V, entrance potential of 8 V and with interface heater on. Selected reaction monitoring (SRM) optimized and fullscan experiments were automatically performed using *LightSight*®. Different kinds of reactions were investigated, such as oxidation, hydroxylation, reduction, C—C bond cleavage, chlorination, and others. During MS/MS experiments, the HPLC analyses were performed as described earlier; however, formic acid was added in the H_2O component of the mobile phase to attain a final concentration of 0.1% (V/V). The injection volume was 20 μL and the samples collected at 0, 1, 2, and 3 h were diluted to one third before the MS/MS analyses.

Short chain carboxylic acids were also determined throughout the electrolysis process by HPLC, using a Rezek ROA-H^{TM} column from Phenomenex® as the stationary phase and 2.5 mM H_2SO_4 as the mobile phase at 0.5 mL min^{-1}. The carboxylic acids (detected at 210 nm) were identified by the comparison of their retention times with those of previously analyzed standards. The injection volume and column temperature were maintained at 25 μL and 23 °C, respectively.

The amount of electrogenerated active chlorine (measured as Cl_2, HOCl, and OCl^-, depending on the solution pH [39]) was monitored by iodometric titration using a standard method [40].

The extent of mineralization (i.e. conversion to CO_2) was monitored by total organic carbon concentration ([TOC]) measurements using a GE Sievers Innovox analyzer. For such, the treated solution was sampled (5 mL) every 1 h. The [TOC] determination was carried out after mixing a diluted volume of the treated sample with H_3PO_4 (6 mol L^{-1}) and $Na_2S_2O_8$ (30% m/V) solutions. The oxidation was accomplished after the temperature and pressure corresponding to the supercritical point of water was reached. The TOC content was analyzed by subtraction of the measured values of inorganic and total carbon, in terms of generated CO_2, and after comparison with a previously determined calibration curve, using a non-dispersive infrared detector.

The mineralization current efficiency (*MCE*) was calculated according to the following equation [41]:

$$MCE = \frac{\Delta[\mathrm{TOC}]_t nFV}{4.32 \times 10^7 mIt} \times 100 \quad (1)$$

where $\Delta[\mathrm{TOC}]_t$ is the measured [TOC] removal (mg L^{-1}) after a certain treatment time, t (h), n the number of exchanged electrons (see Eq. (2)) considering that the applied electric charge was consumed solely by the mineralization process, F the Faraday constant (96,485 C mol^{-1}), V the solution volume (L), 4.32×10^7 is a compounded conversion factor (3600 s h^{-1} × 12,000 mg mol^{-1}), m the number of carbon atoms of the TBT molecule, and I the applied electrical current (A).

$$C_9H_{16}N_4OS(aq) + 33H_2O(l) \rightarrow 9CO_2(g) + 4NO_3{}^-(aq) + SO_4{}^{2-}(aq) + 82H^+(aq) + 76e^- \quad (2)$$

The extent of total electrochemical combustion (φ) [42] was calculated through the ratio between the removal percentages of TBT and TOC each 1 h of treatment for the optimized conditions:

$$\varphi = \frac{\%[\mathrm{TOC}]_{\mathrm{removed}}}{\%[\mathrm{TBT}]_{\mathrm{removed}}} \quad (3)$$

The value of φ gives an indication of the extent of conversion of TBT to CO_2 or to other intermediate compounds. Then, this parameter can assume values between 0 (no combustion) and 1 (complete combustion).

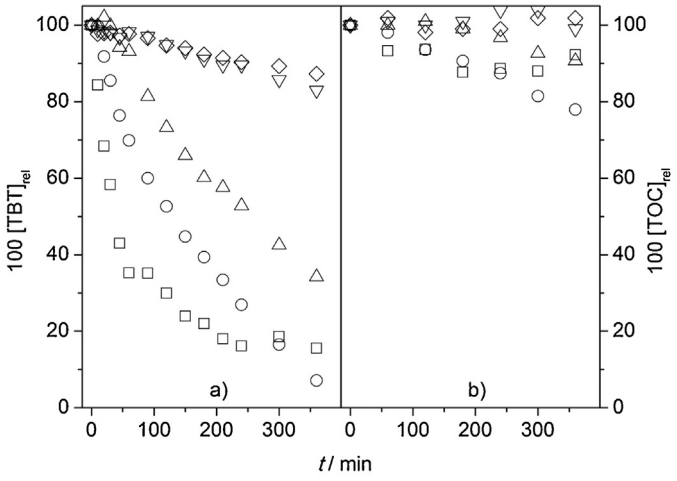

Fig. 1. Relative percentage decay of a) TBT (100 $[\mathrm{TBT}]_{\mathrm{rel}}$) and b) TOC (100 $[\mathrm{TOC}]_{\mathrm{rel}}$) as a function of treatment time for the (□) electrochemical process (using a DSA® anode) and the photochemical process using UVC Hg lamps of distinct power: (○) 125 W, (△) 80 W, (▽) 9 W, and (◊) 5 W. Conditions: 20 mA cm^{-2}, pH 3, 2 g L^{-1} NaCl, and at 25 °C.

The energy consumption per unit TBT mass (w) for the electrochemical and photochemical process was calculated according to [28]:

$$w = \left(\frac{UIt + Pt}{\Delta[\mathrm{X}]V}\right) \quad (4)$$

where U is the cell voltage (V), I the applied electrical current (A), t the reaction time (h), P the nominal power of the Hg lamp (W), Δ[X] the concentration variation of TBT (mg L^{-1}) or TOC (mg L^{-1}) after a certain treatment time, and V the solution volume (L).

3. Results and discussion

3.1. Effect of operational variables

Fig. 1 shows the relative percentage decay of [TBT] (100$[\mathrm{TBT}]_{\mathrm{rel}}$) and [TOC] (100$[\mathrm{TOC}]_{\mathrm{rel}}$) as a function of treatment time for the electrochemical (Hg lamp turned off) and photochemical flow processes (using distinct Hg lamps). Clearly the TBT molecule is significantly oxidized by both the electrochemical and photochemical (80 and 125 W Hg lamps) methods. The use of the low pressure Hg lamps (5 and 9 W) led to poor oxidation performances due to their lower fluency rate compared to those of the high pressure Hg lamps. The oxidation of TBT during the photolysis process might be due to the formation of singlet oxygen ($^1O_2$) [26,27] or HO$^\bullet$ to a lesser extent, under UVC irradiation. In addition, the oxidation process mediated separately by the electrochemical or photochemical methods did not result in significant levels of conversion to CO_2, as can be seen in Fig. 1b, but rather to other intermediates that are more persistent. On the other hand, when those processes are combined, leading to a hybrid electrochemical and photochemical process (HEP process), the oxidation and mineralization rate performances are significantly improved, as can be seen in Fig. 2. The obtained values of the rate constants for the oxidation and mineralization of TBT when distinct UVC lamps were used can be seen in Tables SM 2 and SM 3, in the Supplementary material file. The TBT oxidation rate remained very close for all the Hg lamps used ($k_{1st} \approx 3 \times 10^{-2}$ min^{-1}) in comparison to the separate electrochemical (43.0 L mol^{-1} min^{-1}) and photochemical processes. A change in the reaction order was observed when only the electrochemical process was used. This might indicate that the TBT oxidation mechanism is different when the HEP process is used, as high oxidizing power radicals are generated. During the electrochemical process,

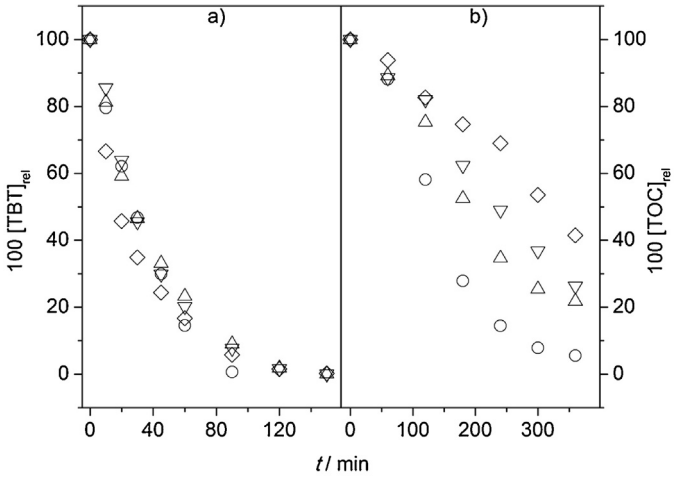

Fig. 2. Relative percentage decay of a) TBT (100 $[TBT]_{rel}$) and b) TOC (100 $[TOC]_{rel}$) as a function of treatment time for the hybrid electrochemical and photochemical process, using UVC Hg lamps of distinct power: (◯) 125 W, (△) 80 W, (▽) 9 W, and (◊) 5 W. Conditions: DSA® anode at 20 mA cm^{-2}, pH 3, 2 g L^{-1} NaCl, and at 25 °C.

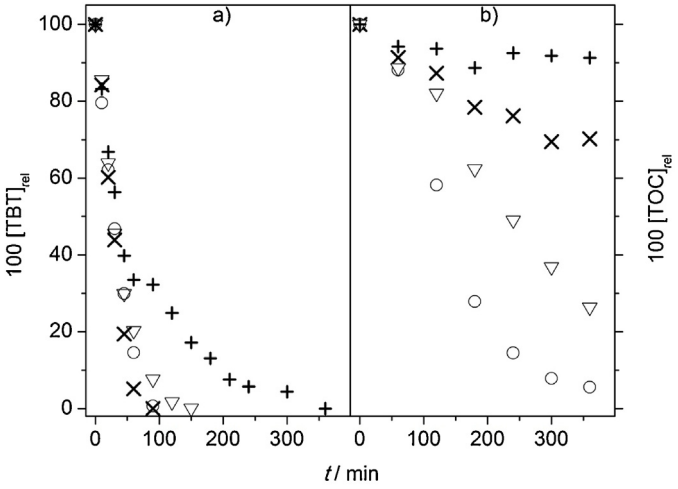

Fig. 3. Experimental and theoretical relative percentage decay of a) TBT (100 $[TBT]_{rel}$) and b) TOC (100 $[TOC]_{rel}$) as a function of treatment time for the hybrid electrochemical and photochemical process using (◯ and ×) 125 W and (▽ and +) 9 W power Hg lamps. The theoretical decays (× and +) of TBT and TOC were obtained as a summation of the relative decays of the electrochemical and photochemical processes separately used (see Figs. SM 2 and SM 3 in the Supplementary material file). Conditions: DSA® anode at 20 mA cm^{-2}, pH 3, 2 g L^{-1} NaCl at 25 °C.

Cl^- ions diffuse towards the surface of the anode and are oxidized, generating Cl_2:

$$Cl^-(aq) \rightarrow Cl(ads) + e^- \quad (5)$$

$$2Cl(ads) \rightarrow Cl_2(aq) \quad (6)$$

The electrogenerated Cl_2 diffuses away from the surface of the anode and might undergo a disproportionation reaction (Eq. (7)) leading to HClO or even OCl^-, depending on the solution pH [43]. The speciation diagram of these species [39,43,44] is dependent on many conditions, such as Cl^- ion concentration, temperature, and ionic strength [45].

$$Cl_2(aq) + H_2O(l) \rightarrow HClO(aq) + Cl^-(aq) + H^+(aq) \quad (7)$$

The HClO species can lead to $HO^\bullet$ and $Cl^\bullet$ by a homolytic homogeneous reaction [22] mediated by UVC radiation (especially at 254 nm) in the bulk of the solution, i.e. without mass transport limitations. Those radicals are responsible for the improvement in the oxidation and mineralization rates of the combined HEP process in comparison to the ones used separately.

In order to confirm whether that improvement is a synergistic effect, i.e. whether other high oxidant species are being produced, the experimental curves for [TBT] and [TOC] decay as a function of treatment time using Hg lamps of 125 W and 9 W were compared with the theoretical ones (obtained by summation of the experimental relative decays of the electrochemical and photochemical processes separately used) as shown in Fig. 3. All the experimental and theoretical curves for [TBT] and [TOC] decay as a function of treatment time for each Hg lamp used in this work can be seen in Figs. SM 2 and SM 3, respectively. It is interesting to note that the experimental and theoretical lines for the relative [TBT] decay are almost equal when using a 125 W Hg lamp, but they are significantly different when using a 9 W Hg lamp. Hence, for the latter case it is possible to confirm the synergistic effect of the combined process, as the experimental line for the HEP process displays superior [TBT] removals than that for the theoretical process. In addition, when the experimental and theoretical lines for the relative [TOC] decay are compared for the distinct Hg lamps used, the beneficial effect of the HEP process on the conversion of organics to CO_2 is markedly impressive. In all situations, the experimental removal levels and rates were higher in comparison to the theoretical ones (the experimental values of the TOC removal rates can be seen in Table SM 3, in the Supplementary material file).

The synergistic effect associated to the hybrid process was also investigated with respect to the concentration of electrogenerated active chlorine (calculated as Cl_2) in the presence and absence of Hg lamps (see Fig. SM 4 in the Supplementary material file). As expected, the amount of Cl_2 produced during the electrochemical process (electrolysis without coupled UVC irradiation) was more than two times higher in comparison to the HEP processes; the maximum faradaic efficiency obtained for the electrochemical process was 29%. Moreover, the Cl_2 concentration decreased as the power of the Hg lamp increased. It is interesting to note that the $[Cl_2]$ evolution was very similar for the HEP processes using Hg lamps of 80 W and 9 W. This might explain the similar removal levels and rates of the HEP processes when these Hg lamps were used, whereas it could also be used to optimize the energy consumption of that process. In this sense, the energy consumption per unit mass (w) as a function of the removal percentage of TBT and TOC for the HEP process using distinct Hg lamps should be compared. As can be seen in Fig. SM 5 in the Supplementary material file, the w values for the removal percentage of TBT and TOC, when using low pressure Hg lamps (5 and 9 W), remained close and around 3 and 10 kW h g^{-1}, respectively, while for the high pressure Hg lamps (80 and 125 W) those values were higher than 10 and 200 kW h g^{-1} for similar levels of TBT and TOC removal, respectively. Clearly, the use of high pressure Hg lamps is not recommended, mainly for TOC removal, because significant excess electric energy is wasted. Sichel et al. [46] already reported on the energy saving potential of the UV/chlorine process when using low pressure Hg lamps of varying power capacities (40 W, 80 W, and 200 W) in comparison to the conventional UV/H_2O_2 advanced oxidation process. Further analyses involve the mineralization current efficiency (MCE) and the electrochemical combustion (φ) for the HEP process as a function of the applied charge per unit volume of treated solution (Q_{ap}). Once again, as can be seen in Fig. SM 6 in the Supplementary material file, the use of a 9 W Hg lamp led to similar MCE (~25%) and φ (~0.7) values in comparison to those for a 80 W Hg lamp, which were slightly lower than the ones for a 125 W Hg lamp ($MCE \sim 27\%$ and $\varphi \sim 1$). It is interesting to point out that this hybrid process exhibited initial MCE values that are comparable to that of Fenton-based advanced oxidation technologies [47–49]. In addition, the conversion to CO_2 was also very high for all tested conditions, which means that one

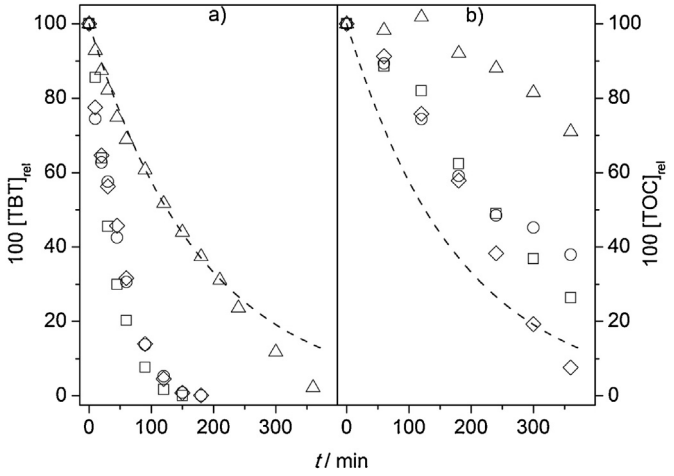

Fig. 4. Relative percentage decay of a) TBT (100 $[TBT]_{rel}$) and b) TOC (100 $[TOC]_{rel}$) as a function of treatment time for the hybrid electrochemical and photochemical process using a 9 W Hg lamp, for distinct pH values: (□) pH 3, (○) pH 7, (△) pH 11, and (◊) no pH control. (– – –) Theoretical line based on a purely mass transport controlled process. Conditions: DSA® anode at 20 mA cm^{-2}, 2 g L^{-1} NaCl at 25 °C.

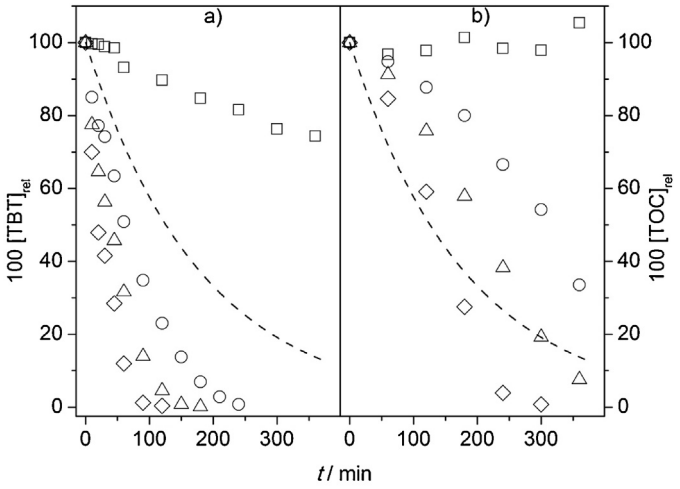

Fig. 5. Relative percentage decay of a) TBT (100 $[TBT]_{rel}$) and b) TOC (100 $[TOC]_{rel}$) as a function of treatment time for the hybrid electrochemical and photochemical process using a 9 W Hg lamp, for distinct NaCl concentrations: (□) 0.0, (○) 1.0, (△) 2.0, and (△) 4.0 g L^{-1}. (– – –) Theoretical line based on a purely mass transport controlled process. Conditions: DSA® anode at 20 mA cm^{-2}, no pH control at 25 °C.

can expect low concentrations of intermediate compounds being generated. Therefore, the investigation of the remaining effects of operational variables was carried out using a 9 W Hg lamp.

Fig. 4 shows the relative percentage decay of TBT and TOC as a function of treatment time for the HEP process at distinct pH values, using a 9 W Hg lamp. As discussed above and taking into account the chlorine species diagram developed in a previous work [39], the predominant active chlorine species in the pH range of 3–7 is HClO. Watts and Linden [50] have already reported on the importance of the different chlorine species being irradiated (particularly HOCl and OCl^-) with UV radiation, as they have different absorbance profiles. As the HOCl species is readily decomposed to $HO^•$ and $Cl^•$ under UV irradiation in an extended wavelength range (around 254 nm) [50], high TBT oxidation rates ($k_{1st} > 2 \times 10^{-2}$ min^{-1}) were attained in the solution bulk (see Table SM 4 in the Supplementary material file) in the pH range of 3–7 (including the condition without control: pH from 6.5 to 3). The data for the mineralization rate exhibited a better fit for zero-order kinetics than for first-or second-order kinetics (see Table SM 5 in the Supplementary material file); a zero-order kinetic process could mean that the conversion to CO_2 is only dependent on the generation of oxidant radicals ($HO^•$ and $Cl^•$) in the bulk of the solution mediated by UVC radiation (the rate determining step), and not on the organic load concentration (this last situation would lead to a mass transport controlled process). As reported by Feng et al. [22], the quantum yield (the ratio of moles of active chlorine decomposed per mole of absorbed photons) of the HOCl decomposition is low; thus the rate equation of the mineralization process (r_{min}) could be approximated as:

$$r_{min} = k_{min}[OL][Ox] = k'_{min} \quad (8)$$

where k_{min} and k'_{min} are second- and zero-order kinetic constants of the mineralization process, respectively, [OL] is the concentration of the organic load, and [Ox] the oxidant concentration, which is dependent on the amount of NaCl used. The low TBT and TOC removal rates in alkaline solutions might be due to the combination of low quantum yield and concentration of the predominant OCl^- species, as discussed by Feng et al. [22], as well as the medium scavenging effect [51] towards $HO^•$. When all these experimental data are compared with a theoretical line purely based on a mass transport process, in which the organic compound needs to diffuse to the electrode surface to be oxidized or mineralized, it is clear that only the data for the TBT oxidation process at pH 11 are similar to the theoretical line (see dashed line in Fig. 4). It is important to highlight that the theoretical and experimental data are related to different oxidation processes, i.e. electrochemical and hybrid processes, respectively. Their comparison is here made only to highlight the importance of the chemical oxidation processes in the bulk of the solution, with no mass transport limitations, compared to a diffusion controlled process (typical of electrochemical systems). Moreover, in the case of TOC removal, it is clear that the experimental points do not show the exponential decay typical of a pseudo-first order kinetic process. The theoretical line was obtained after calculation of the mass transport coefficient (k_m) of the flow reactor used in the experiments, as shown in the work of Coledam et al. [52]. The k_m value was calculated after determination of the thickness of the diffusion layer (2.22×10^{-5} m) by a simple electrochemical assay [53] and determination of the diffusion coefficient of the TBT molecule (8.49×10^{-10} m^2 s^{-1}) using a calibrated diaphragm cell [54].

Fig. 5 shows the relative percentage decay of TBT and TOC as a function of treatment time for the HEP process with a 9 W Hg lamp using distinct [NaCl] values. Clearly, the concentration of Cl^- ions has a significant effect on the TBT and TOC removal rates and levels, because the concentration of active chlorine, and of its decomposition products under UVC irradiation, increase during electrolysis. The oxidation rates of TBT showed a direct relationship with [NaCl], as can be seen in Table SM 6 and Fig. SM 7 in the Supplementary material file. These data confirm that the chemical oxidation process of TBT (k_{COP}) occurring in the bulk of the solution is much faster than the purely electrochemical oxidation of TBT (with no Cl^- ions – see Fig. 5a), the same being true with respect to the theoretical mass transport controlled process. As discussed elsewhere [55], the relationship between the oxidation rate (r_{Ox}) and k_{COP} could be defined as:

$$r_{Ox} = k_{Ox}[Ox][TBT] = k_{COP}[TBT] \quad (9)$$

where k_{Ox} is the kinetic constant for oxidant generation and k_{COP} is the kinetic constant for the chemical oxidation process ($k_{COP} = k_{Ox}[Ox]$). In the case of TOC removal, significant removal levels were attained only in the presence of Cl^- ions (see Fig. 5b), leading to higher conversions to CO_2 as [NaCl] increased, i.e. lower amounts of intermediate compounds are expected to be generated. As discussed earlier, the TOC removal rates for distinct values of [NaCl] exhibited a good fit for a zero-order mineralization reaction

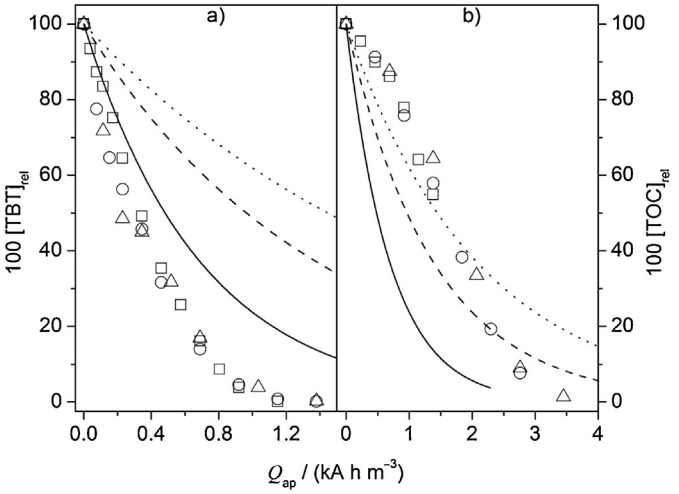

Fig. 6. Relative percentage decay of a) TBT (100 $[TBT]_{rel}$) and b) TOC (100 $[TOC]_{rel}$) as a function of the applied charge per unit volume of treated solution (Q_{ap}) for the hybrid electrochemical and photochemical process using a 9 W Hg lamp, for distinct electric current density values: (□) 10, (○) 20, and (△) 30 mA cm^{-2}. Theoretical lines based on a purely mass transport controlled process using (—)10, (– – –) 20, and (• • •) 30 mA cm^{-2}. Conditions: DSA® anode, 2.0 g L^{-1} NaCl, and no pH control at 25 °C.

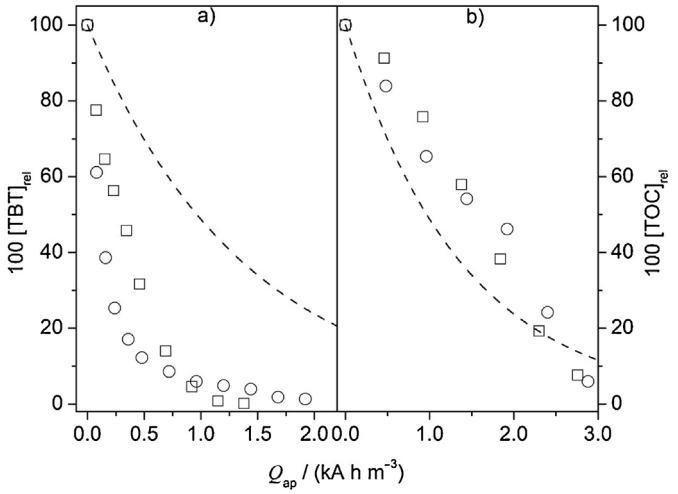

Fig. 7. Relative percentage decay of a) TBT (100 $[TBT]_{rel}$) and b) TOC (100 $[TOC]_{rel}$) as a function of the applied charge per unit volume of treated solution (Q_{ap}) for the (□) hybrid electrochemical and photochemical process (using a DSA® anode) and (○) for the electrochemical process (using a BDD anode). (– – –) Theoretical line based on a purely mass transport controlled process. Conditions: 20 mA cm^{-2}, 2.0 g L^{-1} NaCl, and no pH control at 25 °C.

(see Table SM 7 in the Supplementary material file). Once again, the experimental and theoretical data for the oxidation reaction ([TBT] decay) were very different because this is a much faster process, with only small structural modifications on the TBT molecule resulting in a decrease of its chromatographic signal. On the other hand, those data for the mineralization reaction ([TOC] decay), which is a slower process that must undergo several oxidation steps [55], showed a distinct kinetic behavior, most probably due to the generation of oxidant radicals in the bulk of the solution, as discussed above.

Fig. 6 shows the relative percentage decay of TBT and TOC as a function of the applied charge per unit volume of treated solution (Q_{ap}) for the HEP process with a 9 W Hg lamp using distinct values of current density. Clearly, the oxidation of TBT and the mineralization of TBT and its intermediate compounds do not depend on the applied electrical current. A typical exponential decay behavior was obtained for TBT oxidation, characteristic of a mass transport controlled process. The TBT removal rates higher than the theoretical ones (which exhibited an expected dependence with the applied charge) are due to the increasing generation of active chlorine species and, consequently, to the contribution of the chemical oxidation reaction in the bulk of the solution. This could be confirmed by the linear relationship of the pseudo-first order kinetic constants for TBT oxidation with Q_{ap}, as can be seen in Table SM 8 in Supplementary material file. The TOC decay profile was also very close (similar removal rates) for all tested conditions of applied current density. In addition, contrasting with the case of the TBT oxidation process, the data are close to the theoretical lines. As described above, this might indicate that the oxidation of TBT is leading to intermediate compounds, which are further mineralized to CO_2. The expected fit for pseudo-first order kinetics was very poor in comparison to a zero-order fit, as can be seen in the data of Table SM 9 in the Supplementary material file. All these results were discussed above and are in agreement with the investigation of the reaction order related to TOC abatement for the previously analyzed operational variables.

To assess the performance of the optimized HEP process with a 9 W Hg lamp and a DSA® anode (no pH control of the solution being treated, in the presence of 2.0 g L^{-1} NaCl, and using 20 mA cm^{-2}) considering the oxidation and mineralization of TBT, as well as its energy consumption and *MCE* values, an additional experiment

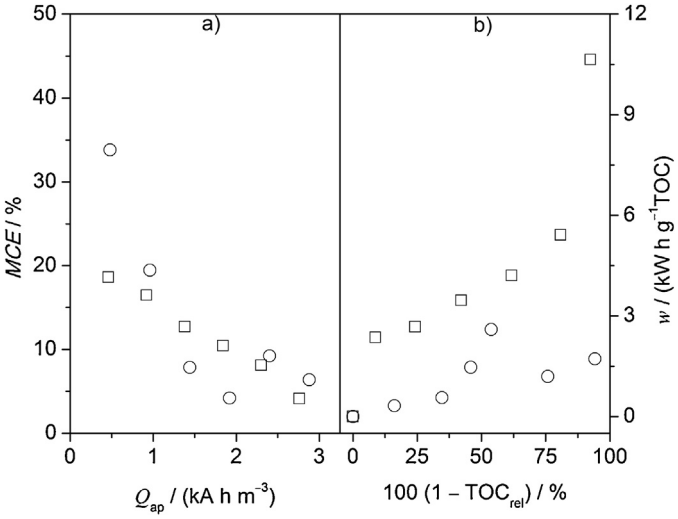

Fig. 8. a) Mineralization current efficiency (*MCE*) as a function of the applied charge per unit volume of treated solution (Q_{ap}) and b) energy consumption per unit mass (w) as a function of the removal percentage of TOC (100 (1–TOC_{rel})) for the (□) hybrid electrochemical and photochemical process (using a DSA® anode) and (○) for the electrochemical process (using a BDD anode). Conditions: 20 mA cm^{-2}, 2.0 g L^{-1} NaCl, and no pH control at 25 °C.

was carried out using a BDD anode at those optimized conditions, but without UVC irradiation. Fig. 7 shows the relative percentage decay of TBT and TOC as a function of Q_{ap} for the HEP process and the electrochemical one using a BDD electrode. Clearly, similar removal percentages and rates were obtained for the oxidation of TBT as well as for the mineralization process. The TBT oxidation rate when using the BDD anode did not exhibit a good mathematical fit for either pseudo-first order or second-order kinetics. On the other hand, the mineralization rate exhibited a good fit for zero-order kinetics, with similar k_{0th} values for the electrochemical and HEP processes: 128 and 142 g L^{-1} min^{-1}, respectively. Despite the similar removal levels and rates, the *MCE* values were slightly higher for the electrochemical process using the BDD electrode than for the HEP process, in the beginning of the treatment. Then, as shown in Fig. 8a, the *MCE* values decreased as the amount of organic load were converted to CO_2 and then remained very close

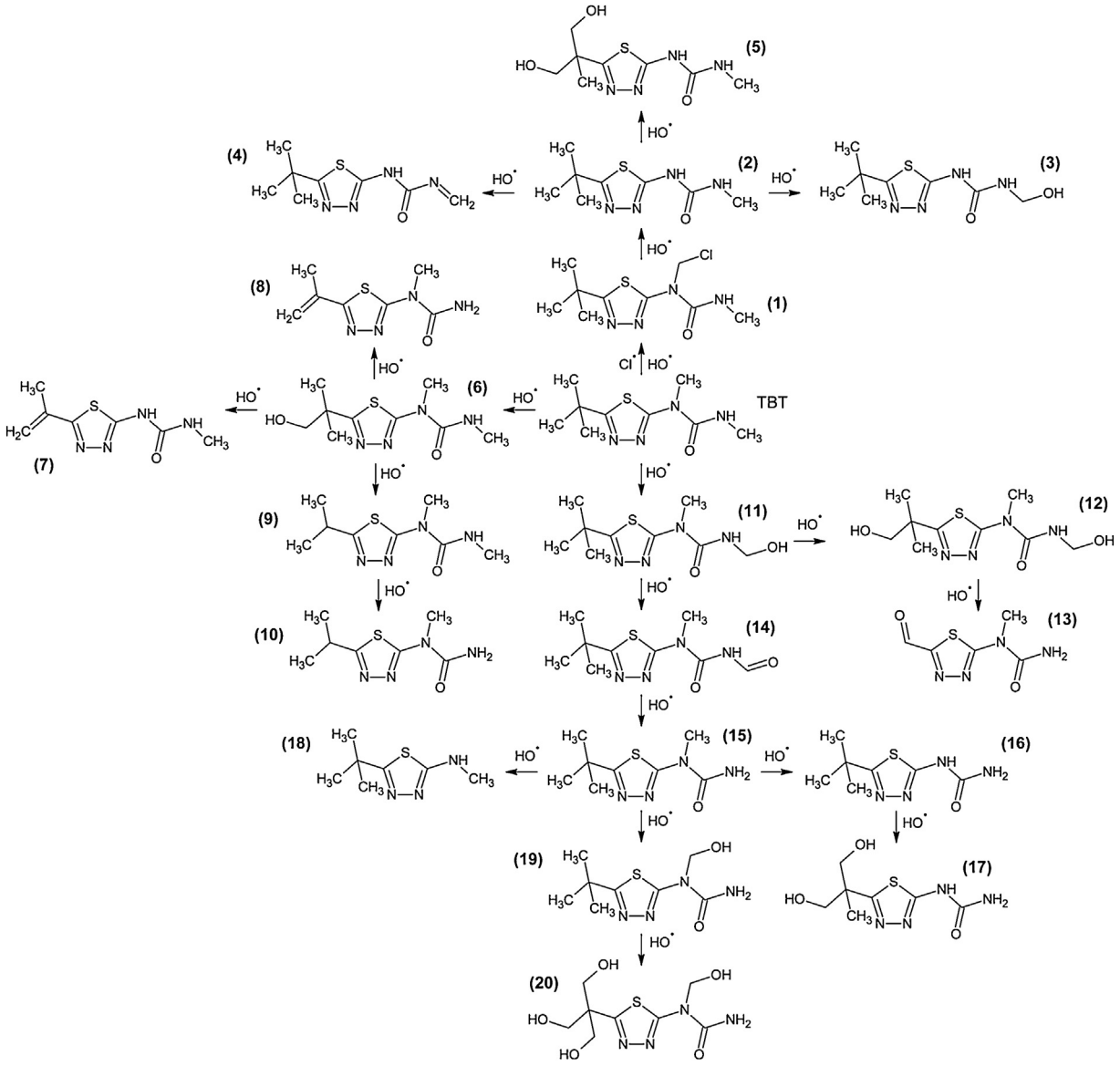

Fig. 9. Possible degradation pathway of the TBT herbicide during a 8 h treatment using the hybrid electrochemical and photochemical process. Conditions: DSA® anode at 20 mA cm^{-2}, 2.0 g L^{-1} NaCl, and no pH control at 25 °C.

for both processes. On the other hand, the extent of total electrochemical combustion was always higher for the HEP process, but it approached 1.0 (complete conversion to CO_2) after 5 h for both processes, as can be seen in Fig. SM8 in the Supplementary material file. The values of the energy consumption per unit mass of TOC removed by the electrochemical and HEP processes (see Fig. 8b) reached around 2 and 12 kW h g^{-1}, respectively, for the almost complete removal of TOC. The higher energy consumption of the HEP process, including with respect to Fenton based processes [48,56], was expected and is due to the use of Hg lamps as already noted by others [57]. It is important to highlight that the *w* values could be reduced if, for example, the faradaic efficiency of the Cl_2 evolution reaction could be increased or more Cl^- ions were added to the treated solution; however, in this latter case intermediate compounds need to be monitored to be sure that no organochlorine is generated. The *w* values for TBT oxidation exhibited a different behavior with respect to those for TOC removal and were equal to 20 and 6 kW h g^{-1} for the electrochemical and HEP processes, respectively, for the almost complete oxidation of TBT (see Fig. SM 9 in the Supplementary material file). In a recent paper, Gozzi et al. [35] used distinct advanced oxidation processes (anodic oxidation with electrogenerated H_2O_2, electro-Fenton, and solar photoelectro-Fenton) to mineralize different solutions containing herbicides, including TBT. Despite the attainment of smaller *w* values (2–5 kW h g^{-1}) for TOC removal using those technologies, the use of the HEP process led to higher TOC removal rate and level, even using a higher initial concentration of TBT.

All these data show that the HEP process could be an interesting option to oxidize and mineralize organic pollutants, if no organochlorine byproduct is generated. Thus, an analysis of intermediate compounds was carried out by LC–MS/MS. The main intermediate compounds, as well as retention times and main fragment ions, detected during a 8 h treatment using the HEP process at the optimal operational conditions can be seen in Table SM 10 in the Supplementary material file. Based on this information, a possible degradation pathway for the initial oxidation steps of TBT is proposed (see Fig. 9). As previously reported by Silva et al. [37], the main detected intermediate compounds resulted from hydroxylation (which indirectly assures the generation of HO•) and oxidation reactions on the central (see compounds **1** and **19**) and terminal

(see compounds **3** and **14**) methyl groups of urea, as well as on the methyl groups of the *tert*-butyl substituent (e.g. compounds **5**, **12**, **13**, **17**, and **20**). Some intermediate compounds resulting from elimination reactions were also observed (see compounds **7** and **8**). These results are in agreement with the literature, as HO$^{\bullet}$ is more effective than Cl$^{\bullet}$ in oxidizing organic molecules [50,58]. In all situations, byproducts from the thiadiazole ring opening were not observed; however, it certainly occurred due to the attained TOC removal. It is also very important to highlight that throughout the 8 h treatment process just one organochlorine compound was detected (compound **1** – m/z 263), which nevertheless was completely eliminated after 3 h of treatment (the evolution of the integrated areas for the main detected intermediate compounds as a function of the treatment time for the HEP process can be seen in Fig. SM 10, in the Supplementary material file).

When short chain carboxylic acids were analyzed, for the HEP process the main detected compounds were tartaric, malic, acetic, butyric, adipic, propionic, and dichloroacetic (DCA) acids. The evolution of the concentration of these carboxylic acids as a function of treatment time can be seen in Fig. SM 11a in the Supplementary material file. After 6 h of treatment using the HEP process, the presence of the DCA acid was no longer quantified (limit of quantification – LOQ = 31.2 μg L^{-1}) or detected. On the other hand, when the analyses were carried out for the electrochemical process using the BDD electrode, the main detected compounds were tartronic, malonic, acetic, DCA, chloroacetic (CA: LOQ = 500 μg L^{-1}) acids. As can be seen in Fig. SM 11b in the Supplementary material file, the concentration of DCA and CA remained low (around 1 and 0.7 mg L^{-1}, respectively), even after 6 h electrolysis. In addition, no signals of the recalcitrant oxalic and oxamic [59] acids were detected during the experiments. The formation of the organochlorine compounds might be due to reactions involving Cl$^{\bullet}$, especially with aliphatic groups [58], which could lead to aliphatic acids.

Considering all the analyzed parameters, clearly the use of the HEP process could be an interesting option to treat effluents containing SOC in the presence of Cl^{-} ions, if a properly adjusted treatment time is used to assure the elimination of organochlorine compounds. Finally, the HEP process using a commercial DSA® anode could also be described as an advanced oxidation process, without limitations to treat acidic solutions.

4. Conclusions

A hybrid electrochemical and photochemical process (using a commercial DSA® anode) was successfully used for the oxidation and mineralization of the herbicide tebuthiuron. The use of a low power Hg lamp (9 W) was sufficient to attain oxidation and mineralization rates comparable to those of a single electrochemical process using a BDD anode. Moreover, a high conversion to CO_2 and comparable *MCE* values with respect to other advanced oxidation processes based on Fenton reactions were attained. On the other hand, slightly higher energy consumptions per unit mass of TOC removed were observed; however, this could be improved if higher concentrations of NaCl could be used or if the electrocatalytic reaction of Cl_2 evolution could be increased. In all these cases, there is the need to monitor the generated byproducts, because the formation of organochlorine compounds is very likely, as observed in this work. All detected intermediate compounds resulted from hydroxylation or oxidation reactions in the distinct methyl groups of TBT; however, no intermediate compound resulting from the rupture of the thiadiazole ring was observed. Additionally, all generated byproducts, including one organochlorine compound, were completely eliminated during the hybrid treatment process, which means that complete conversion to CO_2 was attained. Finally, taking into account all the analyzed parameters, the hybrid electrochemical and photochemical process here reported could be clearly regarded as an advanced oxidation process, without limitations of using acidic solutions, and being an interesting option to treat effluents contaminated with SOC if a proper optimization of the UVC lamp is done.

Acknowledgements

São Paulo Research Foundation (FAPESP – grant numbers 2008/10449-7 and 2016/08124-9), CAPES, and CNPq are gratefully acknowledged for financial support and scholarships. We gratefully acknowledge Professors Romeu C. Rocha-Filho, Sonia R. Biaggio, Nerilso Bocchi, and Luís A. M. Ruotolo for granting access to different apparatuses. ADAMA Brasil is also gratefully acknowledged for supplying samples of the TBT compound.

Appendix A. Supplementary data

Supplementary data associated with this article can be found, in the online version, at http://dx.doi.org/10.1016/j.apcatb.2016.07.003.

References

[1] E.H. Oelkers, J.G. Hering, C. Zhu, Water: is there a global crisis? Elements 7 (2011) 157–162.
[2] E. Brillas, I. Sirés, Electrochemical removal of pharmaceuticals from water streams: reactivity elucidation by mass spectrometry, TrAC rends Anal. Chem. 70 (2015) 112–121.
[3] M.A.F. Locatelli, F.F. Sodré, W.F. Jardim, Determination of antibiotics in Brazilian surface waters using liquid chromatography–electrospray tandem mass spectrometry, Arch. Environ. Contam. Toxicol. 60 (2011) 385–393.
[4] Y. Luo, W. Guo, H.H. Ngo, L.D. Nghiem, F.I. Hai, J. Zhang, S. Liang, X.C. Wang, A review on the occurrence of micropollutants in the aquatic environment and their fate and removal during wastewater treatment, Sci. Total Environ. 473–474 (2014) 619–641.
[5] M. Gavrilescu, K. Demnerová, J. Aamand, S. Agathos, F. Fava, Emerging pollutants in the environment: present and future challenges in biomonitoring, ecological risks and bioremediation, New Biotechnol. 32 (2015) 147–156.
[6] W. Guo, J. Zhang, W. Li, M. Xu, S. Liu, Disruption of iron homeostasis and resultant health effects upon exposure to various environmental pollutants: a critical review, J. Environ. Sci. 34 (2015) 155–164.
[7] I. Oller, S. Malato, J.A. Sánchez-Pérez, Combination of advanced oxidation processes and biological treatments for wastewater decontamination—a review, Sci. Total Environ. 409 (2011) 4141–4166.
[8] K. Singh, S. Arora, Removal of synthetic textile dyes from wastewaters: a critical review on present treatment technologies, Crit. Rev. Environ. Sci. Technol. 41 (2011) 807–878.
[9] I. Sirés, E. Brillas, M.A. Oturan, M.A. Rodrigo, M. Panizza, Electrochemical advanced oxidation processes: today and tomorrow. A review, Environ. Sci. Pollut. Res. 21 (2014) 8336–8367.
[10] F. Sopaj, M.A. Rodrigo, N. Oturan, F.I. Podvorica, J. Pinson, M.A. Oturan, Influence of the anode materials on the electrochemical oxidation efficiency. Application to oxidative degradation of the pharmaceutical amoxicillin, Chem. Eng. J. 262 (2015) 286–294.
[11] A. El-Ghenymy, F. Centellas, R.M. Rodríguez, P.L. Cabot, J.A. Garrido, I. Sirés, E. Brillas, Comparative use of anodic oxidation, electro-Fenton and photoelectro-Fenton with Pt or boron-doped diamond anode to decolorize and mineralize Malachite Green oxalate dye, Electrochim. Acta 182 (2015) 247–256.
[12] B.C. Lourencao, R.A. Medeiros, O. Fatibello-Filho, Simultaneous determination of antihypertensive drugs by flow injection analysis using multiple pulse amperometric detection with a cathodically pretreated boron-doped diamond electrode, J. Electroanal. Chem. 754 (2015) 154–159.
[13] A. Fabiańska, A. Ofiarska, A. Fiszka-Borzyszkowska, P. Stepnowski, E.M. Siedlecka, Electrodegradation of ifosfamide and cyclophosphamide at BDD electrode: decomposition pathway and its kinetics, Chem. Eng. J. 276 (2015) 274–282.
[14] A. Kapałka, G. Fóti, C. Comninellis, The importance of electrode material in environmental electrochemistry: formation and reactivity of free hydroxyl radicals on boron-doped diamond electrodes, Electrochim. Acta 54 (2009) 2018–2023.
[15] J.M. Aquino, G.F. Pereira, R.C. Rocha-Filho, N. Bocchi, S.R. Biaggio, Electrochemical degradation of a real textile effluent using boron-doped diamond or b-PbO_2 as anode, J. Hazard. Mater. 192 (2011) 1275–1282.
[16] R.B.A. Souza, L.A.M. Ruotolo, Electrochemical treatment of oil refinery effluent using boron-doped diamond anodes, J. Environ. Chem. Eng. 1 (2013) 544–551.

[17] S. Trasatti, Electrocatalysis: understanding the success of DSA®, Electrochim. Acta 45 (2000) 2377–2385.
[18] H. Olvera-Vargas, N. Oturan, E. Brillas, D. Buisson, G. Esposito, M.A. Oturan, Electrochemical advanced oxidation for cold incineration of the pharmaceutical ranitidine: mineralization pathway and toxicity evolution, Chemosphere 117 (2014) 644–651.
[19] F.L. Souza, J.M. Aquino, D.W. Miwa, M.A. Rodrigo, A.J. Motheo, Electrochemical degradation of dimethyl phthalate ester on a DSA® electrode, J. Braz. Chem. Soc. 25 (2014) 492–501.
[20] G.R.P. Malpass, D.W. Miwa, A.C.P. Miwa, S.A.S. Machado, A.J. Motheo, Study of photo-assisted electrochemical degradation of carbaryl at dimensionally stable anodes (DSA®), J. Hazard. Mater. 167 (2009) 224–229.
[21] G. Li, M. Zhu, J. Chen, Y. Li, X. Zhang, Production and contribution of hydroxyl radicals between the DSA anode and water interface, J. Environ. Sci. 23 (2011) 744–748.
[22] Y. Feng, D.W. Smith, J.R. Bolton, Photolysis of aqueous free chlorine species (HOCl and OCl^-) with 254 nm ultraviolet light, J. Environ. Eng. Sci. 6 (2007) 277–284.
[23] Z. Ye, H. Zhang, X. Zhang, D. Zhou, Treatment of landfill leachate using electrochemically assisted UV/chlorine process: effect of operating conditions, molecular weight distribution and fluorescence EEM-PARAFAC analysis, Chem. Eng. J. 286 (2016) 508–516.
[24] G. Hurwitz, P. Pornwongthong, S. Mahendra, E.M.V. Hoek, Degradation of phenol by synergistic chlorine-enhanced photo-assisted electrochemical oxidation, Chem. Eng. J. 240 (2014) 235–243.
[25] D. Nasuhoglu, V. Yargeau, D. Berk, Photo-removal of sulfamethoxazole (SMX) by photolytic and photocatalytic processes in a batch reactor under UV-C radiation (max = 254 nm), J. Hazard. Mater. 186 (2011) 67–75.
[26] D. Vione, D. Bagnus, V. Maurino, C. Minero, Quantification of singlet oxygen and hydroxyl radicals upon UV irradiation of surface water, Environ. Chem. Lett. 8 (2010) 193–198.
[27] A.L. Boreen, B.L. Edhlund, J.B. Cotner, K. Mcneill, Indirect photodegradation of dissolved free amino acids: the contribution of singlet oxygen and the differential reactivity of DOM from various sources, Environ. Sci. Technol. 42 (2008) 5492–5498.
[28] J.M. Aquino, K.N. Parra, D.W. Miwa, A.J. Motheo, Removal of phthalic acid from aqueous solution using a photo-assisted electrochemical method, J. Environ. Chem. Eng. 3 (2015) 429–435.
[29] S. Aquino Neto, A.R. De Andrade, Electrochemical degradation of glyphosate formulations at DSA® anodes in chloride medium: an AOX formation study, J. Appl. Electrochem. 39 (2009) 1863–1870.
[30] I.C. Eleotério, J.C. Forti, A.R. De Andrade, Electrochemical treatment of wastewater of veterinary industry containing antibiotics, Electrocatalysis 4 (2013) 283–289.
[31] C. Lourencetti, M.R.R. de Marchi, M.L. Ribeiro, Determination of sugar cane herbicides in soil and soil treated with sugar cane vinasse by solid-phase extraction and HPLC-UV, Talanta 77 (2008) 701–709.
[32] M.L.M. Tagert, J.H. Massey, D.R. Shaw, Water quality survey of Mississippi's upper pearl river, Sci. Total Environ. 481 (2014) 564–573.
[33] S.A. Alves, T.C.R. Ferreira, M.R.V. Lanza, Electrochemical oxidation of the herbicide tebuthiuron using DSA®-type electrode, Quim. Nova 35 (2012) 1981–1984.
[34] S.A. Alves, T.C.R. Ferreira, N.S. Sabatini, A.C.A. Trientini, F.L. Migliorini, M.R. Baldan, N.G. Ferreira, M.R.V. Lanza, A comparative study of the electrochemical oxidation of the herbicide tebuthiuron using boron-doped diamond electrodes, Chemosphere 88 (2012) 155–160.
[35] F. Gozzi, I. Sirés, A. Thiam, S.C. de Oliveira, A.M. Junior, E. Brillas, Treatment of single and mixed pesticide formulations by solar photoelectro-Fenton using a flow plant, Chem. Eng. J. (2016) http://dx.doi.org/10.1016/j.cej.2016.1002.1026.
[36] M.R.A. Silva, A.G. Trovó, R.F.P. Nogueira, Degradation of the herbicide tebuthiuron using solar photo-Fenton process and ferric citrate complex at circumneutral pH, J. Photochem. Photobiol. A 191 (2007) 187–192.
[37] M.R.A. Silva, W. Vilegas, M.V.B. Zanoni, R.F.P. Nogueira, Photo-Fenton degradation of the herbicide tebuthiuron under solar irradiation: iron complexation and initial intermediates, Water Res. 44 (2010) 3745–3753.
[38] R.F.P. Nogueira, M.R.A. Silva, A.G. Trovó, Influence of the iron source on the solar photo-Fenton degradation of different classes of organic compounds, Sol. Energy 79 (2005) 384–392.
[39] J.M. Aquino, R.C. Rocha-Filho, N. Bocchi, S.R. Biaggio, Electrochemical degradation of the Disperse Orange 29 dye on a β-PbO_2 anode assessed by the response surface methodology, J. Environ. Chem. Eng. 1 (2013) 954–961.
[40] A.D. Eaton, L.S. Clesceri, A.E. Greenberg, Standard Methods for the Examination of Water and Wastewater, 19th ed., United Book Press, Baltimore, 1995.
[41] E. Brillas, I. Sirés, M.A. Oturan, Electro-Fenton process and related electrochemical technologies based on Fenton's reaction chemistry, Chem. Rev. 109 (2009) 6570–6631.
[42] D.W. Miwa, G.R.P. Malpass, S.A.S. Machado, A.J. Motheo, Electrochemical degradation of carbaryl on oxide electrodes, Water Res. 40 (2006) 3281–3289.
[43] C.Y. Cheng, G.H. Kelsall, Models of hypochlorite production in electrochemical reactors with plate and porous anodes, J. Appl. Electrochem. 37 (2007) 1203–1217.
[44] D.P. Cherney, S.E. Duirk, J.C. Tarr, T.W. Collette, Monitoring the speciation of aqueous free chlorine from pH 1 to 12 with Raman spectroscopy to determine the identity of the potent low-pH oxidant, Appl. Spectrosc. 60 (2006) 764–772.
[45] T.X. Wang, D.W. Margerum, Kinetics of reversible chlorine hydrolysis: temperature dependence and general-acid/base-assisted mechanisms, Inorg. Chem. 33 (1994) 1050–1055.
[46] C. Sichel, C. Garcia, K. Andre, Feasibility studies: UV/chlorine advanced oxidation treatment for the removal of emerging contaminants, Water Res. 45 (2011) 6371–6380.
[47] B.R. Garza-Campos, J.L. Guzmán-Mar, L.H. Reyes, E. Brillas, A. Hernández-Ramírez, E.J. Ruiz-Ruiz, Coupling of solar photoelectro-Fenton with a BDD anode and solar heterogeneous photocatalysis for the mineralization of the herbicide atrazine, Chemosphere 97 (2014) 26–33.
[48] A.M.S. Solano, S. Garcia-Segura, C.A. Martínez-Huitle, E. Brillas, Degradation of acidic aqueous solutions of the diazo dye Congo Red by photo-assisted electrochemical processes based on Fenton's reaction chemistry, Appl. Catal. B 168–169 (2015) 559–571.
[49] F.C. Moreira, S. Garcia-Segura, R.A.R. Boaventura, E. Brillas, V.J.P. Vilar, Degradation of the antibiotic trimethoprim by electrochemical advanced oxidation processes using a carbon-PTFE air-diffusion cathode and a boron-doped diamond or platinum anode, Appl. Catal. B 160–161 (2014) 492–505.
[50] M.J. Watts, K.G. Linden, Chlorine photolysis and subsequent OH radical production during UV treatment of chlorinated water, Water Res. 41 (2007) 2871–2878.
[51] D. Wang, J.R. Bolton, R. Hofmann, Medium pressure UV combined with chlorine advanced oxidation for trichloroethylene destruction in a model water, Water Res. 46 (2012) 4677–4686.
[52] D.A.C. Coledam, J.M. Aquino, R.C. Rocha-Filho, N. Bocchi, S.R. Biaggio, Influence of chloride-mediated oxidation on the electrochemical degradation of the Direct Black 22 dye using boron-doped diamond and β-PbO_2 anodes, Quim. Nova 37 (2014) 1312–1317.
[53] P. Cañizares, J. García-Gómez, I.F. de-Marcos, M.A. Rodrigo, J. Lobato, Measurement of mass-transfer coefficients by an electrochemical technique, J. Chem. Educ. 83 (2006) 1204–1207.
[54] A.R. Gordon, The diaphragm cell method of measuring diffusion, Ann. N.Y. Acad. Sci. 46 (1945) 285–308.
[55] J.M. Aquino, R.C. Rocha-Filho, C. Sáez, P. Cañizares, M.A. Rodrigo, High efficiencies in the electrochemical oxidation of an anthraquinonic dye with conductive-diamond anodes, Environ. Sci. Pollut. Res. 21 (2014) 8442–8450.
[56] N. Barhoumi, L. Labiadh, M.A. Oturan, N. Oturan, A. Gadri, S. Ammar, E. Brillas, Electrochemical mineralization of the antibiotic levofloxacin by electro-Fenton-pyrite process, Chemosphere 141 (2015) 250–257.
[57] E. Brillas, A review on the degradation of organic pollutants in waters by UV photoelectro-Fenton and solar photoelectro-Fenton, J. Braz. Chem. Soc. 25 (2014) 393–417.
[58] L.H. Nowell, J. Hoigné, Photolysis of aqueous chlorine at sunlight and ultraviolet wavelengths—II. Hydroxyl radical production, Water Res. 26 (1992) 599–605.
[59] S. Garcia-Segura, E. Brillas, Mineralization of the recalcitrant oxalic and oxamic acids by electrochemical advanced oxidation processes using a boron-doped diamond anode, Water Res. 45 (2011) 2975–2984.